SEMARAK ILMU PUBLISHING

Journal of Advanced Research in Applied Sciences and Engineering Technology

Journal homepage:
https://semarakilmu.com.my/journals/index.php/applied_sciences_eng_tech/index
ISSN: 2462-1943

Effects of High-Density Polyethylene (HDPE) and Additives Fuel Blends on Diesel Engine's Performance and Emissions and NOx Prediction using Boosted Tree Model

Mohammad Nor Khasbi Jarkoni[1], Muhammad Afiq Danial Ramli[1], Wan Nurdiyana Wan Mansor[1,2,3,*], Che Wan Mohd Noor[1,2], Sheikh Alif Ali[1,2], Anuar Abu Bakar[1,2], Nurul Huda Abd Kadir[3,5], Mohamad Adan Yusof[3,6], How-Ran Chao[4]

[1] Faculty of Ocean Engineering Technology, Universiti Malaysia Terengganu, 21300 Kuala Nerus, Terengganu, Malaysia
[2] Fuel and Engines Research Interest Group, Universiti Malaysia Terengganu, 21300 Kuala Nerus, Terengganu, Malaysia
[3] Syngas Research Interest Group, Universiti Malaysia Terengganu, 21300 Kuala Nerus, Terengganu, Malaysia
[4] Department of Environmental Science and Engineering, College of Engineering, National Pingtung University of Science and Technology, Pingtung County 912, Taiwan
[5] Faculty of Science and Marine Environment, Universiti Malaysia Terengganu, 21300 Kuala Nerus, Terengganu, Malaysia
[6] Syngas Sdn. Bhd., Gong Badak Industrial Zone, 21300 Kuala Nerus, Terengganu, Malaysia

ABSTRACT

The rising demand for eco-friendly and sustainable fuel options has prompted the investigation of alternative energy sources. This study explores the use of blends of High-Density Polyethylene (HDPE), and 7% biodiesel (B7) with additives as a substitute for diesel fuel. The research involves comparing three different mix ratios of HDPE and additives with a conventional B7 blend: a control of 100% B7, a mix of 90% B7 with 10% HDPE, and a blend of 85% B7 with 10% HDPE and 5% additives. Fourier Transform Infrared (FTIR) spectroscopy was employed to identify the fuels' functional groups. The study also measured key performance metrics, including brake-specific fuel consumption (BSFC), brake power (BP), and exhaust emissions of nitrogen oxides (NO_x), carbon monoxide (CO), hydrocarbons (HC), and carbon dioxide (CO_2). A Boosted Tree Model was used to establish a prediction and analysis of NO_x emissions. The findings indicate that incorporating additives into the HDPE blend positively influences both engine performance and emissions. The combination of HDPE and additives with B7 resulted in reduced emissions across various engine loads and speeds, decreasing hydrocarbon and carbon-containing emissions. The Boosted Tree Model, with a configuration of 4 leaf nodes, demonstrated strong predictive accuracy, with a coefficient of determination (R^2) of 0.86 and a root-mean-square error (RMSE) of 0.38 for the training dataset, and R^2 of 0.97 with RMSE of 0.16 for the validation dataset. The study underscores the benefits of integrating HDPE and additives into diesel blends, highlighting their potential to lower emissions and supporting the search for viable alternative fuels.

Keywords:

Plastic fuel; Additives; Biodiesel; Pyrolysis; Engine's emission and performance; Boosted tree

[*] *Corresponding author.*
E-mail address: nurdiyana@umt.edu.my

https://doi.org/10.37934/araset.54.2.269286

1. Introduction

The advent of plastic has revolutionized countless aspects of human life, from packaging and consumer goods to sophisticated medical devices and aerospace components [1]. Its durability, lightweight nature, and versatility have made plastic an indispensable material in modern society. However, the very properties that make plastic so valuable also contribute to a growing environmental crisis. The issues surrounding plastic use and disposal have become increasingly complex, highlighting the need for sustainable management and innovation. One of the primary concerns with plastic is its significant contribution to global pollution. Plastics, particularly single-use items like bags, bottles, and straws, often end up in landfills, oceans, and other natural environments [2].

Due to their non-biodegradable nature, these materials can persist for hundreds to thousands of years, posing a severe threat to wildlife, marine ecosystems, and, indirectly, human health. Animals can ingest or become entangled in plastic waste, leading to injury or death, while microplastics, tiny plastic particles, have been found in water sources, food supplies, and even the air we breathe, with unknown long-term health effects [3]. Moreover, the production of plastic is resource-intensive, relying heavily on fossil fuels. From extraction to processing, the lifecycle of plastic contributes significantly to carbon emissions and climate change [3,4].

New developments in chemical recycling techniques, such as pyrolysis, provide some optimism in light of this challenge. Pyrolysis is a process that transforms plastic waste into a usable energy source, breaking down the long-chain polymers of plastic into smaller, more manageable molecules in the absence of oxygen. High temperatures, usually between 300 and 900 °C, are applied to plastic trash, which causes it to disintegrate into smaller hydrocarbon molecules [5]. The absence of oxygen prevents combustion and allows the material to undergo chemical changes through thermal decomposition. The resulting product of the pyrolysis process can be a liquid fuel, gas, or solid residue, depending on the specific conditions and the type of plastic used [4]. The liquid fuel produced through this process is often referred to as plastic fuel or plastic-derived fuel. Plastic fuel can be used in place of conventional petroleum-based fuels like gasoline, diesel, or natural gas [6]. It can be further refined, combined with regular fuels, or utilized as a single fuel in a variety of industries, such as industrial, power, and transportation.

The pyrolysis of HDPE between 500 and 800 °C to create liquid fuel oil, gaseous products, and solid char in the presence of nitrogen has been used as an inert carrier gas and the ideal temperature to achieve the highest oil product yield (70%) was 550 °C [4]. Previous study shows that diesel engines use waste plastic oil to provide stability in performance and efficiency [6]. Plastic fuel can be blended with conventional fuels such as diesel or gasoline and can be used in several applications such as transportation, industrial processes, and power generation [7-10].

Parallel to plastic-derived fuels, biodiesel presents another renewable alternative, produced from vegetable oils or animal fats. It is chemically like petroleum diesel and can be used in unmodified diesel engines. Biodiesel is typically blended with petroleum diesel in varying percentages, depending on the desired fuel properties and emissions standards. Biodiesel can be used in a variety of vehicles, including cars, trucks, buses, and heavy equipment. It can also be used in heating oil and as a feedstock for jet fuel. Nowadays biodiesel is the most important alternative diesel fuel in the EU representing 82% of the total biofuel production [11].

Fuel additives play a crucial role in optimizing fuel properties without extensive modifications to existing engine technologies. These additives are substances that can be added or blended to the fuel to alter the properties of the fuel and give us better results without making any major changes to the current engine technology. Fuel additives are a cost-effective way of addressing the issues associated

with the use of biodiesel in diesel engines. It can be added to lubricating, diesel, and petrol oils to enhance engine operation and efficiency. The addition of additives to biodiesel gives better performance for the engine [12,13]. For example, the additives, cetane booster can improve the cetane number of diesel fuel and enhance the combustion efficiency of the engine.

Previous studies showed that the addition of additives to the diesel fuel emits less CO emission [14]. The higher oxygen concentration of additives enhanced CO oxidation and reduced CO emissions. Higher level of HC emissions was also found in the mixture of B7 and HDPE [15]. With the higher oxygen content in the additives, it helps for the more complete combustion resulting in the decrease of HC emission. The higher emissions of CO_2 associated with B7 fuel were linked to the oxygen content of biodiesel fuel and its lower carbon content [8]. However, the blended fuel with the additives emits higher NO_x because the cetane improver decreases the ignition delay at the earlier start of the combustion process shifting in-cylinder temperature and pressure causing higher NO_x emissions [16].

In this study, the performance of a single diesel engine and its emissions, including NO_x, CO, HC, and CO_2, were investigated. The fuels' spectrum properties were examined using the Fourier Transform Infrared (FTIR) spectroscopy method. The use of machine learning techniques was carried out, with a specific emphasis on creating a boosted tree model-based NO_x emission prediction model. The boosted tree model, an advanced ensemble method in machine learning, enhances prediction accuracy by integrating multiple weak models into a stronger and more reliable one. Software tools were utilized to process and analyse a comprehensive dataset, including fuel properties, combustion performance, emissions, and other relevant characteristics. This method aligns with previous research, which has demonstrated the effectiveness of deep learning and machine learning techniques in accurately predicting vehicle emissions models [17,18].

2. Methodology

2.1 Overall framework

The study followed four main steps as shown in Figure 1. First, it collected HDPE from Syngas Sdn Bhd and processed it through pyrolysis to turn it into fuel. An additive was mixed into the fuel in storage tanks to improve its properties, with the amount controlled and the mixture stirred well for even distribution.

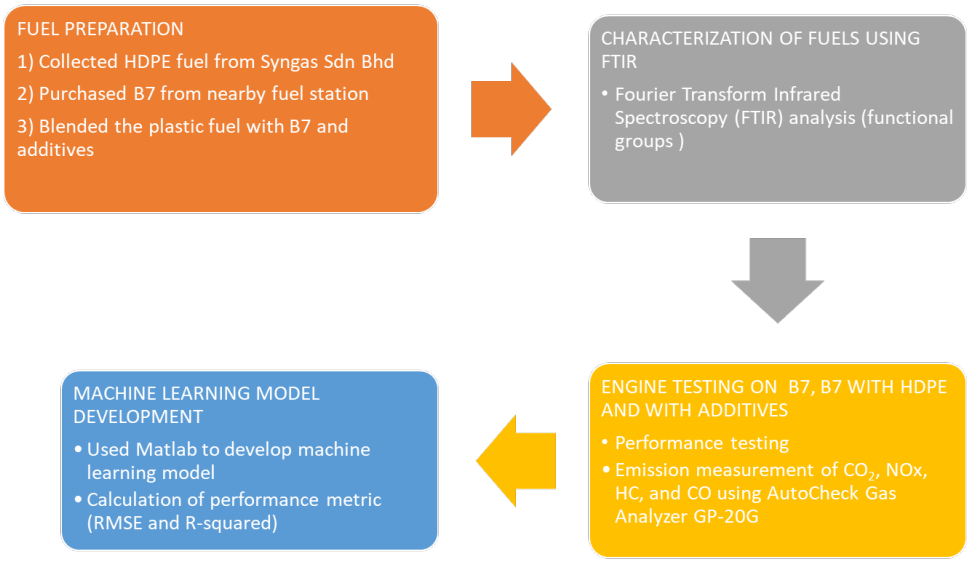

Fig. 1. Framework of the study

Three different fuel blends, named Fuel 1, Fuel 2, and Fuel 3, were prepared in specific amounts as listed in Table 1. Then, the diesel fuels were characterized using FTIR. The FTIR analysis was conducted using a Bruker FTIR spectrometer from 400 to 4000 cm^{-1} with an average resolution of 4 cm^{-1}. IR radiation was passed through a sample to identify the functional groups present in the diesel fuel. For engine testing, all sensors or instruments used to collect data were calibrated, and safety protocols were verified. Baseline testing was conducted to establish the engine's initial performance characteristics. This baseline testing involved Fuel 1, followed by Fuel 2 and 3.

Table 1
The mixing ratio of the fuels

Label	Fuel	Ratio by volume (1 Liter)
Fuel 1	Biodiesel (B7)	100
Fuel 2	B7, HDPE	90:10
Fuel 3	B7, HDPE, and Additives (cetane booster)	85:10:5

Figure 2 shows the fuel used in this study.

Fig. 2. The fuel blends in the laboratory diesel engine

Figure 3 shows the photograph of Bruker FTIR spectrometer, located at Universiti Malaysia Terengganu. Engine speed, torque, and fuel consumption at various load conditions were investigated using a Yanmar diesel engine.

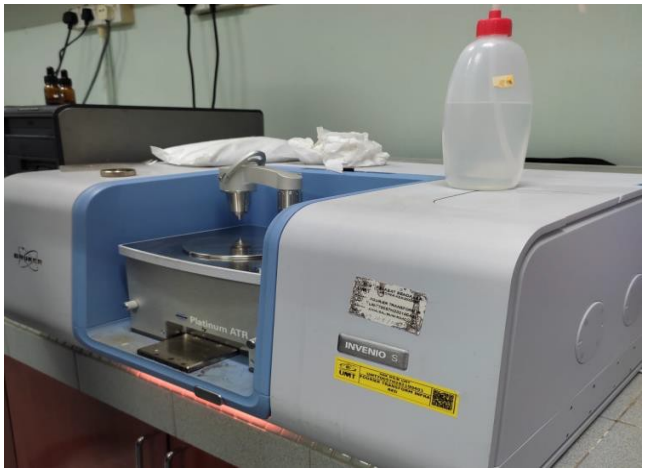

Fig. 3. Photograph of Bruker FTIR spectrometer

2.2 Engine Testing

A baseline testing was conducted to establish the engine's initial performance characteristics. Fuel 1 is the baseline for this study. Engine speed, torque, and fuel consumption at various load conditions were investigated using a Yanmar diesel engine. The engine was coupled with an eddy current dynamometer for torque and load measurements. The schematic diagram and specification of the diesel engine are illustrated in Figure 4 and Table 2, respectively.

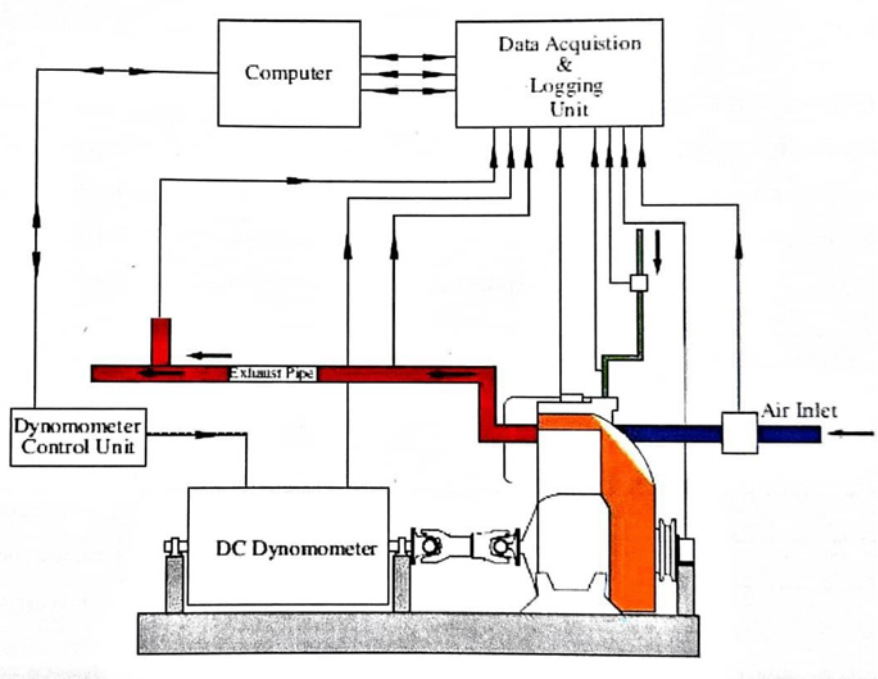

Fig. 4. Engine schematic diagram

Table 2
Engine specifications

Item	Specification
Type	Yanmar L48N6-MTMYI 4 strokes, single-cylinder, diesel engine
Bore X Stroke	(70 X 57) mm
Displacement	0.219 liter
Cooling system	Air-cooled
Oil Tank Capacity	2.4 liter
Rated Output	3.1 kW
Rated Speed	3000 rpm

The photographs of the engine are shown in Figure 5, where it displays sensors and instrument locations.

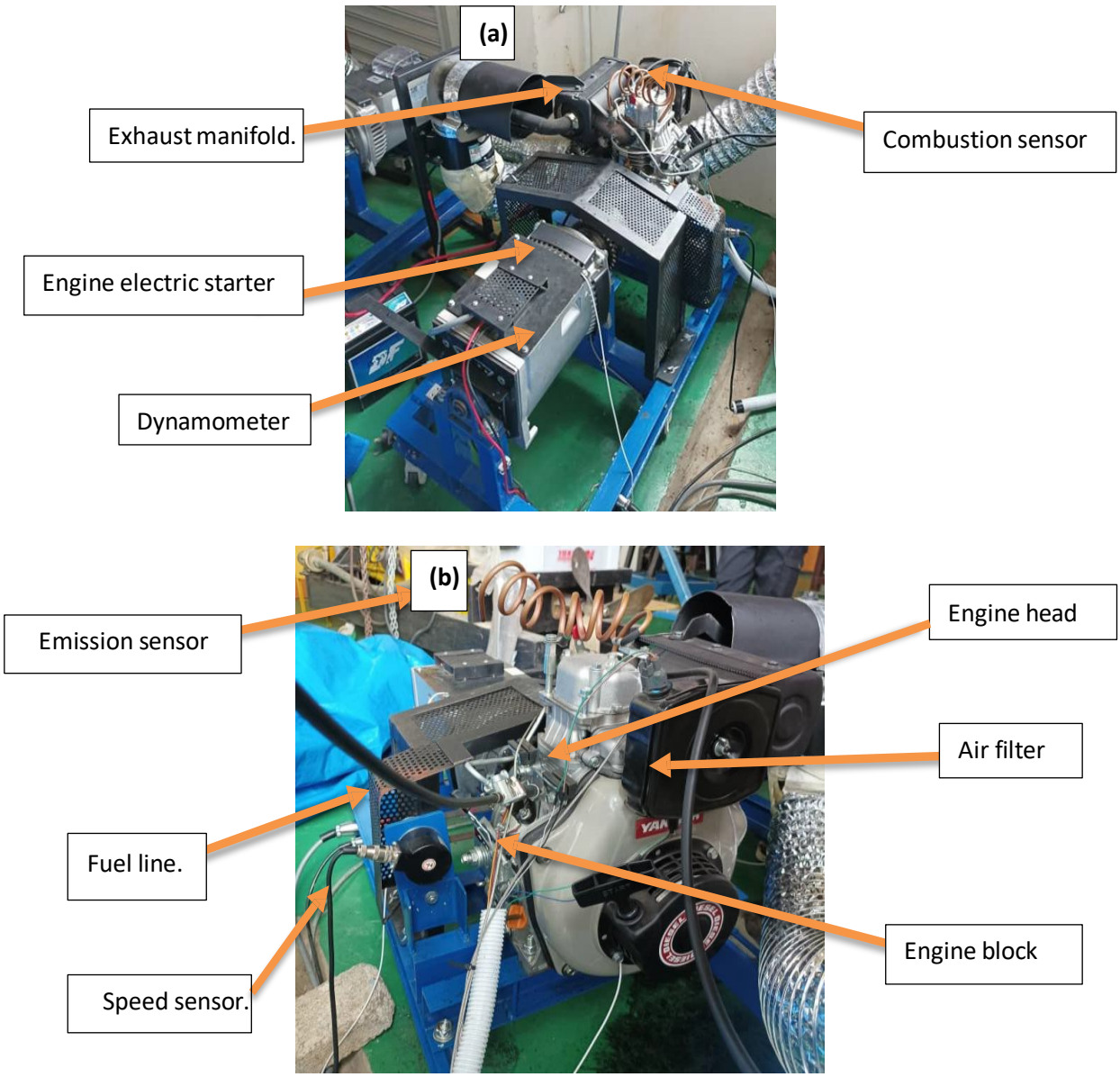

Fig. 5. Labelling of Yanmar L48N6-MTMYI Diesel Engine in (a) and (b)

The performance and combustion data were recorded using Dyno Monitor and Combustion Analysis Model CAS-5 software. This combustion analysis system included a crank angle encoder with a Top Dead Centre (TDC) trigger, an in-cylinder pressure transducer and amplifier, and a data acquisition unit (DAQ) to measure the combustion pressure. To determine cylinder pressure, the pressure transducer monitored diaphragm deflection. It was an optical type sensor, which offered a very consistent signal in contrast to piezoelectric sensors, known to wander over time. The encoder crank angle signal provided the clock for the DAQ, to which each pressure data point correlated. This simplified data processing as compared to time-based DAQ systems.

Table 3
Engine testing conditions for all tests

Item	Specification				
Torque load (%)	100	75	50	25	12
Weighting factor	0.05	0.25	0.30	0.30	0.10
Fuel labels	Fuel 1, Fuel 2 and Fuel 3				
Speed (rpm)	2000 ± 20 and 3000 ± 20				

An AutoCheck Gas Analyzer GP-20G was used for emission measurement of CO, HC, NO_x, and CO_2. In this experiment, two types of software—Dynamometer and Focus Combustion Analysis System—were employed. The engine's torque and speed were read from or controlled by the Dynamometer software. It displays information about the engine's performance, such as engine speed, load applied, BSFC, and BP. Information concerning combustion data was provided via the Focus Combustion Analysis System Software [19]. The system is shown in Figure 6.

Fig. 6. Combustion Analysis Model CAS-5

The AutoCheck Gas Analyzer GP-20G was used to measure the emissions from the samples. This device analysed the concentrations of gases, including NO_x, CO_2, HC, CO, and O_2 by employing infrared radiation absorption. Different gases absorbed the infrared radiation at specific wavelengths, enabling precise measurement and identification of the individual gases within the emissions. To ensure accuracy across various speeds and loads during the testing, the filter of the analyser was periodically changed. The analyser is shown in Figure 7.

Fig. 7. Autochek Gas Analyzer GP-20G

The experiment is carried out under steady-state conditions. This condition is achieved when the intake manifold temperature reaches 43 ± 1°C and the block coolant temperature reaches 88 ± 1°C. Throughout the experiment, the engine speed is held constant at 2000 ± 20 rpm and repeated for a second speed at 3000 ± 20 rpm. To prevent coke formation in the fuel, the fuel return temperature after the fuel cooler is kept as near to the fuel inlet temperature as possible. The ISO 8178 Type D2 for constant speed engine, non-road test cycle with various weighting factors is used for steady-state engine testing and exhaust measurement. The weighting factors, torque load, speed, and corresponding power used in this study are presented in Table 3. The start of injection (SOI) timing is controlled by the engine ECU, which is left in its default setting. The engine is put into stabilization for 15 minutes once a steady state has been achieved before data is logged. Emission analysers then recorded data for a duration of 10 minutes. To analyse combustion, data were gathered three times for every 1000 engine cycles, with 50 cycles deemed sufficient for robust analysis [7]. Additionally, data on fuel flow were collected at three separate instances within every two-minute interval.

To assess the engine's fuel efficiency, BSFC was calculated. BSFC represents the rate of fuel consumption relative to the power output of the engine. It is a critical metric for understanding how efficiently an engine converts fuel into usable work. The calculation of BSFC was conducted using Eq. (1). BP is a fundamental parameter used to assess the performance of an engine under various operating conditions, providing valuable insights into its efficiency and power delivery capabilities. The BP was determined using Eq. (2). It is typically measured using a dynamometer, which applies a load to the engine to simulate real-world conditions. The conversion from exhaust gas emissions in (ppm and vol%) to BSFC (g/KW.hr) is shown in Eq. (3) till [20,21].

$$BSFC = \frac{Fuel\ Consumption\left(\frac{g}{hour}\right)}{Brake\ Power\ (kW)} \quad (1)$$

$$BP = \frac{2\pi\ x\ Speed\ (rpm) x\ Torque\ (Nm)}{60\ x\ 1000} \quad (2)$$

$$CO\ (g/KW.hr) = 3.591 \times 10^{-3} \times CO\ (ppm) \quad (3)$$

$$CO_2\ ((g/KW.hr) = 63.47 \times CO_2\ (vol\ \%) \quad (4)$$

$$HC\ (g/KW.hr) = 2.002 \times 10^{-3} \times HC\ (ppm) \quad (5)$$

NO_x (g/KW.hr) = 6.636 x 10^{-3} x NO_x (ppm) (6)

O_2 (g/KW.hr) = 41.024 x O_2 (vol %) (7)

2.3 Machine Learning (Boosted Tree)

The prediction task used the Matlab Regression Learner app with boosted trees as the preferred algorithm. Boosted trees were chosen for their ability to handle non-linear relationships and complex interactions within the data. As shown in Figure 8, the dataset was split into training and testing sets with a ratio of 70% for training and 30% for testing.

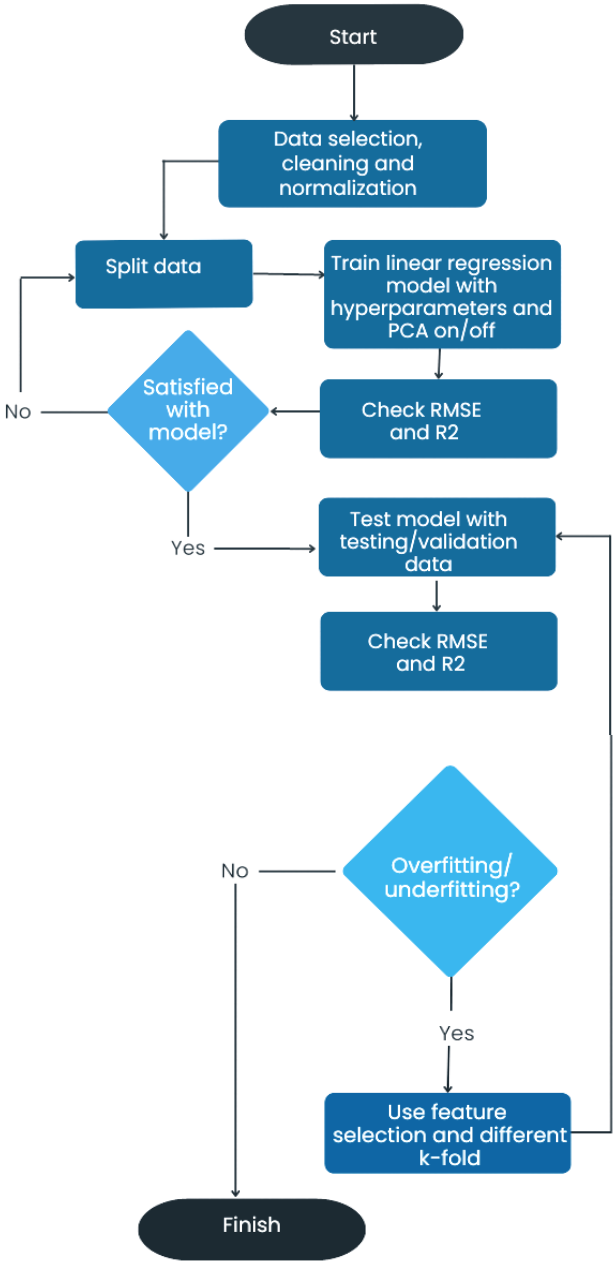

Fig. 8. Flowchart of prediction development using Boosted Tree Model

The procedural framework for model development, illustrated in Figure 9, began with data selection, followed by data cleaning and normalization processes to ensure data quality and consistency. To ensure the accuracy and robustness of the models, K-fold cross-validation was employed, with commonly chosen values of 5 and 10 for the K-fold parameter [8]. Additionally, feature selection, robust regression, and Principal Component Analysis (PCA) with 95% variance explained were conducted to assess their impact on the model's performance.

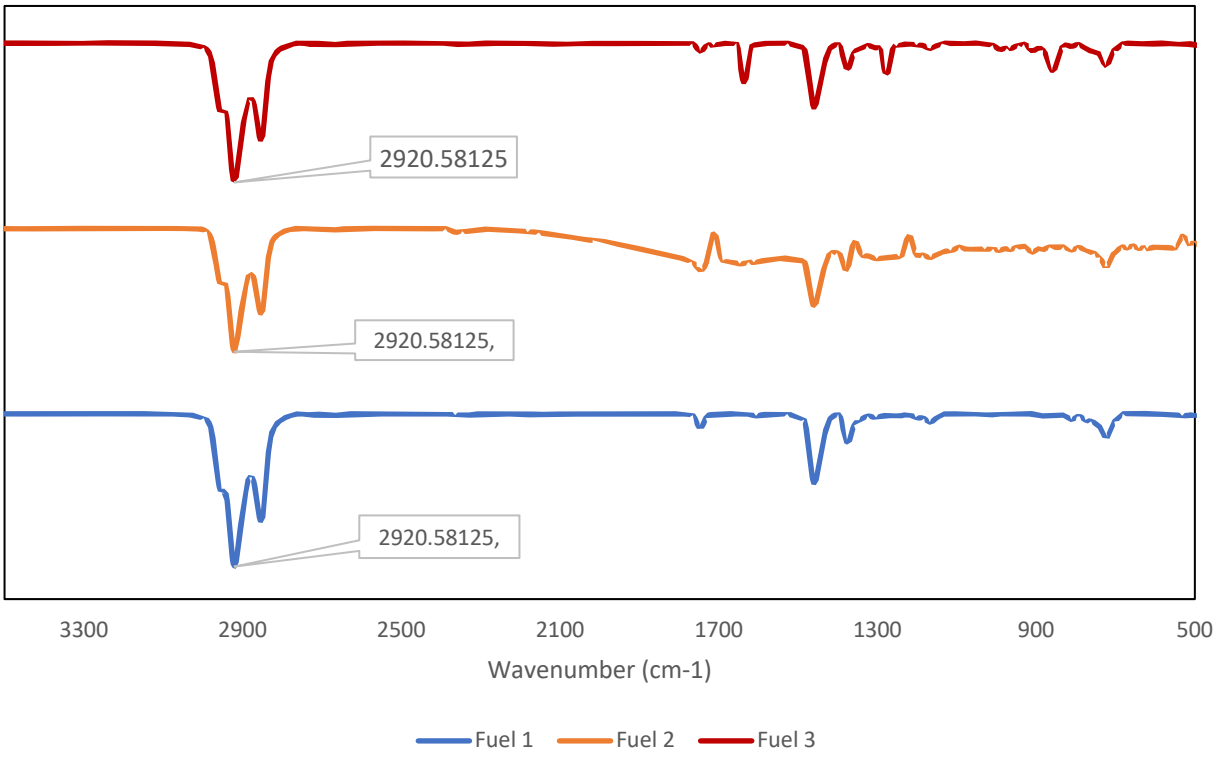

Fig. 9. Functional group of the fuels

Model performance was evaluated using key metrics, including R-squared or Coefficient of Determination (R^2) and Root Mean Square Error (RMSE), serving as indicators of goodness of fit [11]. The trained model was then tested using the remaining validation and testing data. Subsequent re-evaluation of R^2 and RMSE was performed, and the results were compared with those obtained during the model training phase. If significant deviations were observed, feature selection techniques were employed to reduce the difference between parameters.

3. Results and Discussion

3.1 Data of FTIR Analysis

Figure 9 depicts the infrared absorption spectra of three distinct fuel blends resulting from the combination of B7, B7 & HDPE, and B7, HDPE & additives. Within the spectra of these fuel blends and their respective mixtures, characteristic absorption bands were observed. These bands reveal similarities in the functional groups and chemical bonds present across all fuel blends. Notably, two prominent absorptions were observed at 2920 cm^{-1} and 2850 cm^{-1}, corresponding to the asymmetric and symmetrical stretches of CH3, CH2, and CH groups, indicative of aliphatic carbons [22]. Another distinctive absorption band at 1746 cm^{-1} was solely observed for Fuel 1 (baseline), attributed to the

stretching of the C=O double bond in the carbonyl group. Well-defined peaks at 1458 cm^{-1} were identified, attributed to the flexion of deformation experienced by the C-H bond. However, Fuel 3 exhibited slightly unique absorption characteristics compared to the others. Notably, two absorption bands were observed at 1274 cm^{-1} and 857 cm^{-1}, corresponding to the deformation of C-O and bending vibration of C-C, respectively [23]. Further elucidation of the observed peaks in this region is provided in Table 4.

Table 4
Fourier Transform Infrared (FTIR) peak description

Item	Specification
2920	Asymmetric stretch of CH, CH2, CH3
2850	The symmetric stretch of CH, CH2, CH3
1746	Stretch of Carbonyl group bond C=O
1458	Asymmetric deformation of the bonds CH, CH2, CH3
1274	Deformation of the bond C-O
857	Bending Vibration of C-C
721	Bending Vibration of CH2

3.2 Data of BSFC

Figure 10 illustrates the BSFC decreased as the speed increased. Notably, at 3000 rpm, the BSFC was lower than at 2000 rpm. Incomplete combustion occurs in an engine running at low load because of several variables including reduced cylinder pressure, longer combustion interval, and inefficient utilization of air and fuel [24,25]. The maximum BSFC reading occurred at 2000 rpm with a 10% load, where Fuel 3 recorded the highest value at 1254.85 g/kW.hr, representing a 11.63% increase compared to Fuel 1 at 1124.14 g/kW.hr, and a 24.15% decrease compared to Fuel 2 at 852.64 g/kW.hr. Conversely, the lowest BSFC reading was recorded at 3000 rpm with a 100% load. Fuel 3 exhibited the lowest BSFC at 78.66 g/kW.hr, surpassing both the baseline and Fuel 2 readings, which were 82.21 g/kW.hr and 81.14 g/kW.hr, respectively. The higher readings of BSFC for Fuel 3, compared to the baseline and Fuel 2 primarily attributed to its higher energy density and incomplete combustion, which reduce the overall combustion efficiency. Conversely, at the highest speeds, the BSFC value is lowest, owing to the enhanced conversion efficiency of the fuel during the combustion process [24].

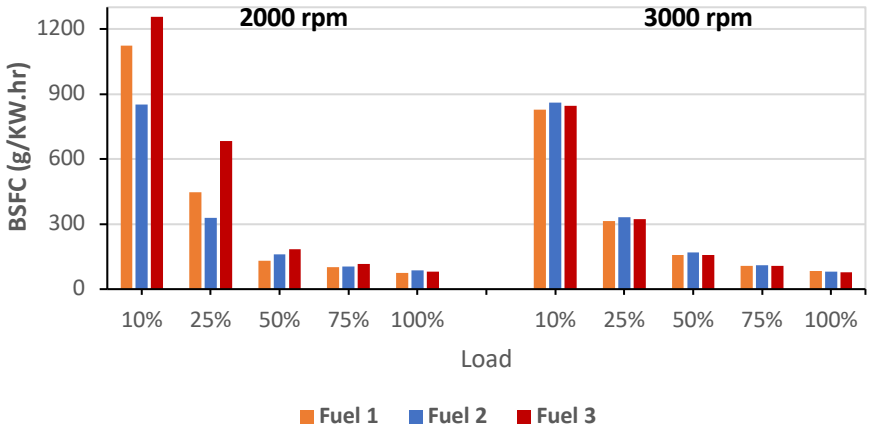

Fig. 10. BSFC for Fuel 1,2 and 3 at various loads and speeds

3.3 Data of BP

In Figure 11, the results of all tested fuels are presented. As depicted, there is a noticeable increase in BP with increasing speed. Specifically, at 3000 rpm, the BP is higher than at 2000 rpm. The maximum BP reading was recorded at 3000 rpm with a 100% load, where Fuel 2 exhibited a value of 3.2137 kW, surpassing the baseline by almost 2% at 3.1523 kW and Fuel 3 by over 1.5% at 3.1620 kW. Conversely, the lowest BP measurement was obtained at 2000 rpm and a 10% load. For Fuel 2, this measurement yielded a value of 0.2209 kW, which was higher than the baseline and Fuel 3 readings, which stood at 0.2143 kW and 0.2106 kW respectively. The higher BP readings for Fuel 2 compared to the baseline and Fuel 3 can be attributed to the higher crankshaft speed (r/min) during the experimental diesel engine operation.

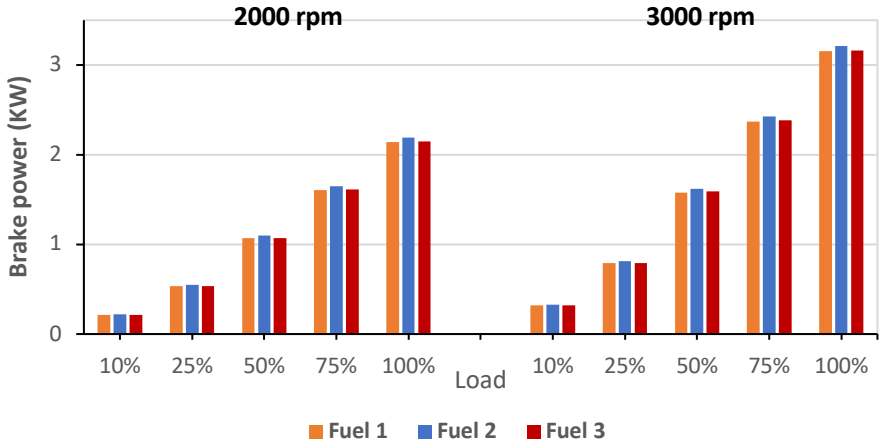

Fig. 11. BP for Fuel 1,2 and 3 at various loads and speeds

3.4 Data of Emission

3.4.1 Emissions of CO

Based on the data depicted in Figure 12, it is evident that the emission of CO decreases as the engine speed increases across all tested fuels. Specifically, CO emissions at 2000 rpm are higher compared to those at 3000 rpm. The maximum CO reading was recorded at 2000 rpm for Fuel 2, while the minimum reading was recorded at 3000 rpm for Fuel 3. Moreover, Fuel 2 exhibited the highest CO emissions at both 2000 rpm and 3000 rpm compared to Fuel 1 and Fuel 3. Conversely, at both 2000 rpm and 3000 rpm, Fuel 3 exhibited the lowest CO emissions among all tested fuels.

At 2000 rpm and 100% load, the CO emission reading for Fuel 2 (0.000286 g/kW.hr) was higher than that for Fuel 1 (0.000247 g/kW.hr) and Fuel 3 (0.000144 g/kW.hr). This observation aligns with previous findings, indicating that the higher CO emissions for Fuel 2 are attributed to its blended composition, which possesses higher viscosity. This higher viscosity can lead to poor atomization within the combustion chamber, resulting in incomplete combustion [26]. Additionally, the aromatic content present in the blended fuel can increase ignition delay and reduce the length of combustion, further contributing to elevated CO emissions. Overall, these findings underscore the importance of fuel composition in influencing emission characteristics, with blended fuels potentially leading to higher CO emissions due to their unique properties affecting combustion dynamics.

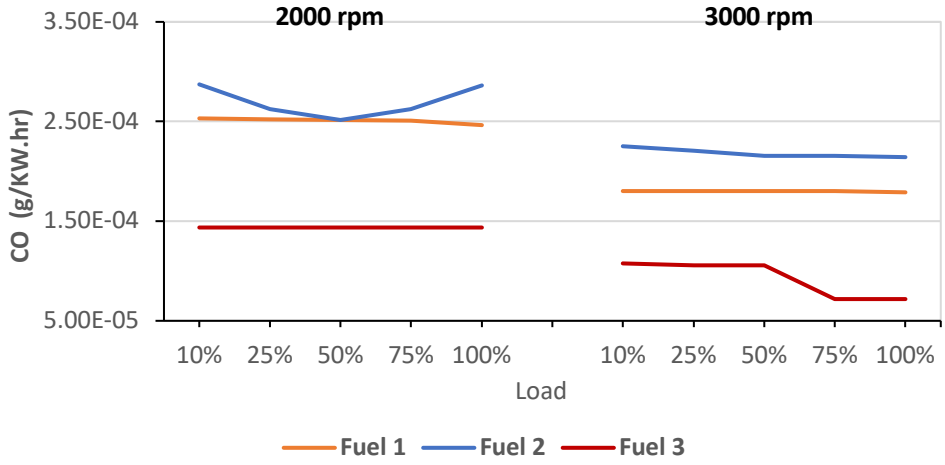

Fig. 12. CO emission for Fuel 1,2 and 3 at various loads and speeds

3.4.2 Emissions of CO_2

According to the data presented in Figure 13, there is a notable trend of increasing CO_2 emissions as engine speeds rise across all tested fuels. Specifically, CO_2 emissions at 3000 rpm were higher compared to those at 2000 rpm. The highest CO_2 reading was recorded at 3000 rpm for baseline fuel, while the lowest reading was recorded at 2000 rpm for Fuel 2. Notably, CO_2 emissions were lowest Fuel 2 at both 2000 rpm and 3000 rpm compared to other fuels. At 2000 rpm, CO_2 emissions tended to decrease from 10% load to 100% load for all blended fuels. However, at 3000 rpm, there was a tendency for CO_2 emissions to decrease from 10% load to 100% for Fuel 3, while the opposite trend was observed for Fuel 1 and 2, where CO_2 emissions remained constant at 108.0048 g/kW.hr. Nevertheless, this value was the highest among all tested fuels. The higher readings of CO_2 emissions for Fuel 1 compared to 2 and 3 can be attributed to the higher oxygen content in Fuel 1. This higher oxygen content can enhance fuel combustion, leading to increased CO_2 emissions [13].

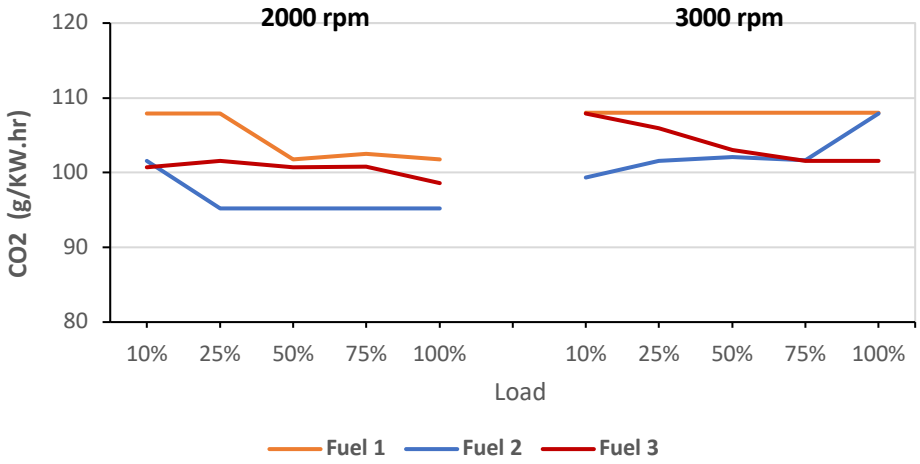

Fig. 13. CO_2 emission for Fuel 1,2 and 3 at various loads and speeds

3.4.3 Emissions of HC

According to the data depicted in Figure 14, there is a consistent trend of decreasing HC emissions as engine speeds increase across all tested fuels. HC emissions were notably higher at 2000 rpm

compared to 3000 rpm. The highest HC reading was recorded at 2000 rpm with a 100% load, measuring 0.0570 g/kW.hr for Fuel 2, while the lowest reading was also recorded at 2000 rpm with a 10% load, measuring 0.0125 g/kW.hr for Fuel 3. At both 2000 rpm and 3000 rpm, Fuel 2 consistently emitted higher HC emissions compared to Fuel 1 and Fuel 3. Conversely, HC emissions were lowest for Fuel 3 at both 2000 rpm and 3000 rpm compared to other fuels. The higher HC emissions observed for Fuel 2 compared to the baseline and Fuel 3 can be attributed to the lower cetane number of the pyrolyzed fuel. This lower cetane number can slow down ignition and result in incomplete combustion [26]. When combustion is not fully realized, it can lead to higher HC emissions being released into the environment.

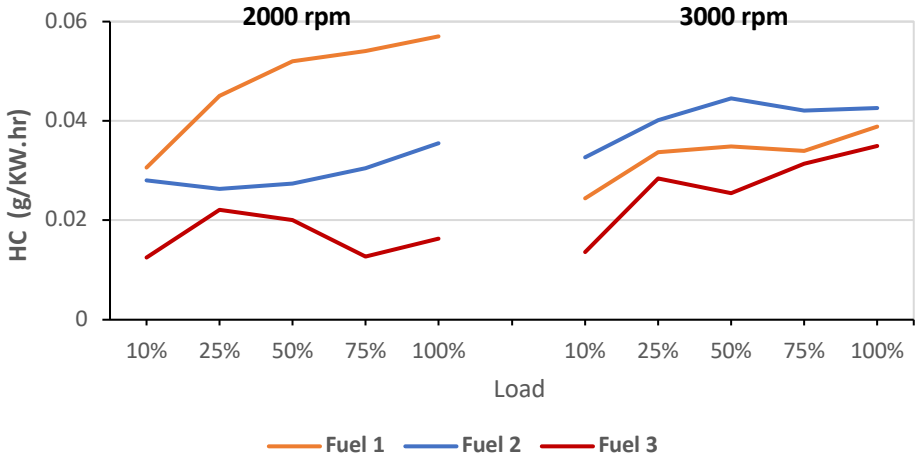

Fig. 14. HC emission for Fuel 1,2 and 3 at various loads and speeds

3.4.4 Emissions of NO_x

By the findings presented in Figure 15, which depict decreasing NO_x emissions as engine speeds increase across all tested blended fuels, there is a complementary relationship observed with HC emissions. Specifically, at 2000 rpm, where NO_x emissions were notably higher than at 3000 rpm, there was a corresponding trend of elevated HC emissions. This relationship is particularly evident in the case of Fuel 3, which emitted the highest NO_x emissions at both 2000 rpm and 3000 rpm, while also exhibiting the highest HC emissions. The inverse relationship between NO_x and HC emissions suggests a complex interplay between combustion parameters and fuel properties. For instance, the observed increase in NO_x emissions at lower engine speeds may be attributed to the conditions favouring thermal NO_x formation, which occurs at high temperatures during combustion [27]. This phenomenon is exacerbated by the presence of certain fuel additives, such as cetane boosters, which can accelerate the combustion process, leading to higher temperatures and increased NO_x production. Conversely, at higher engine speeds, where NO_x emissions decrease, there tends to be a corresponding decrease in HC emissions [28]. This could be attributed to improved combustion efficiency at higher speeds, resulting in more complete combustion of hydrocarbon fuel molecules and consequently reduced HC emissions.

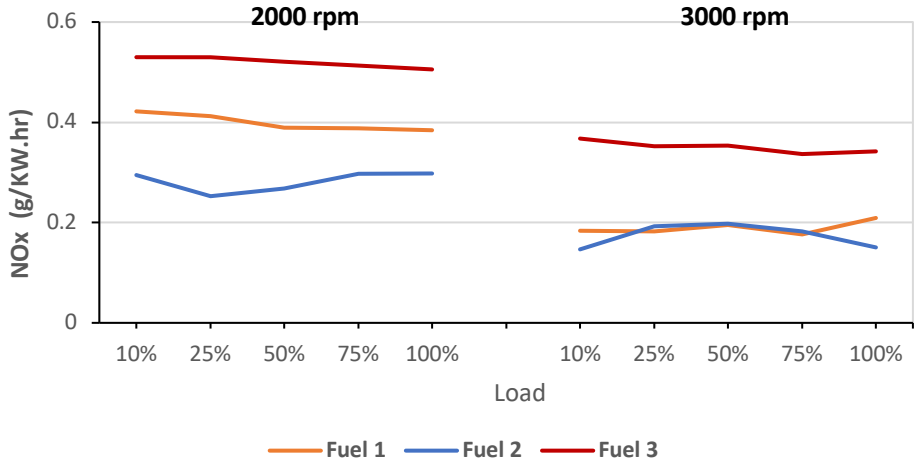

Fig. 15. NO_x emission for Fuel 1,2 and 3 at various loads and speeds

3.5 MatLab Prediction (Boosted Tree Model)

The results obtained from the Boosted Trees Model, as presented in Table 5, indicate promising predictive performance for NO_x emissions. Among the models tested, Model No. 4 stands out as particularly effective in predicting NO_x emissions, achieving a remarkably low RMSE of 0.16 and a high R^2 of 0.97 on the testing dataset. This suggests that Model No. 4, trained with a minimum leaf size of 4 and 20 learners, demonstrates strong predictive capabilities for NO_x emissions [28]. Consequently, it could serve as a valuable tool for accurately forecasting NO_x levels in various scenarios, contributing to improved environmental monitoring and management efforts. The variations in hyperparameters, such as the minimum leaf size and number of learners, directly influence the model's ability to capture the underlying patterns in the data. For instance, reducing the minimum leaf size from 8 to 4 (Model No. 2 to Model No. 4) leads to a notable improvement in both RMSE and R^2 values, indicating enhanced predictive accuracy and model fit. Additionally, the testing results provide insights into the generalization capabilities of the models. Model No. 4, with a minimum leaf size of 4 and 20 learners, stands out with significantly lower RMSE and higher R^2 values on the testing dataset compared to other models. This suggests that Model No. 4 not only performs well on the training dataset but also demonstrates robustness in predicting NO_x emissions on unseen data, indicating its potential for real-world applications.

Table 5
Prediction models for NO_x using the Boosted Tree method

Boosted Trees Model		Hyperparameter	Training (70%)		Tested (30%)	
Model	Minimum leaf size	Numbers of learners	R^2	RMSE	R^2	RMSE
2	8	30	0.76	0.49	0.90	0.31
3	6	25	0.86	0.37	0.91	0.29
*4	4	20	0.86	0.38	0.97	0.16
5	2	10	0.76	0.49	0.87	0.36

4. Conclusions

For FTIR analysis, it is possible to highlight and identify that all the blended fuels have similar structural characteristics. However, the infrared spectrum of all blended fuels does not have hydroxyl groups and no absorption is presented in the fingerprint region, showing an absence of O-H bonds.

The 3000rpm speed showed lower BSFC than the 2000rpm speed for all tested fuel. As we can see, the BSFC for Fuel 2 was higher than for Fuel 1 and Fuel 3. It is because the fuel had higher energy density and incomplete combustion that can affect the combustion efficiency. Other than that, the 3000rpm speed showed higher BP than the 2000rpm speed for all blended fuel. As we can see, Fuel 2 also has the highest BP than Fuel 1 and Fuel 3. This happened during the engine diesel experiment we obtained the highest speed of the fuel. Based on the formula of BP, as the crankshaft speed (r/min) rises, the BP also increases, generating more power output for the engine

In terms of emissions, the CO, HC, and NO_x decrease as the speed of load increases. Fuel 2 emitted the highest CO and HC emissions than other fuels because the highest viscosity and lowest cetane number can produce the highest CO and HC. The CO_2 was higher for Fuel 1 than other fuels because of the higher oxygen content that contributes to the CO_2 emissions. Lastly, Fuel 3 showed that the fuel emitted the highest NO_x emissions. This is because the additive that blended with the fuel had a cetane improver that shifted in-cylinder temperature and pressure in the combustion chamber, releasing the higher NO_x.

The Boosted Tree model showed the effective predictive modelling of the result. The results give model No. 4 achieved the best analysis and allow accurate predictions of the NO_x emissions that the gap between R^2 for training data and R^2 for testing data which are 0.86% and 0.97% respectively.

Acknowledgment
This research was funded by the Talent and Publications Enhancement Research Grant (TAPE-RG) of University Malaysia Terengganu TAPERG/2023/UMT/2142

References

[1] Ibrahim, Idowu David, Yskandar Hamam, Emmanuel Rotimi Sadiku, Julius Musyoka Ndambuki, Williams Kehinde Kupolati, Tamba Jamiru, Azunna Agwo Eze, and Jacques Snyman. "Need for sustainable packaging: an overview." *Polymers* 14, no. 20 (2022): 4430. https://doi.org/10.3390/polym14204430

[2] Kumar, Rakesh, Anurag Verma, Arkajyoti Shome, Rama Sinha, Srishti Sinha, Prakash Kumar Jha, Ritesh Kumar *et al.,* "Impacts of plastic pollution on ecosystem services, sustainable development goals, and need to focus on circular economy and policy interventions." *Sustainability* 13, no. 17 (2021): 9963. https://doi.org/10.3390/su13179963

[3] Gabisa, Elias W., Chavalit Ratanatamskul, and Shabbir H. Gheewala. "Recycling of plastics as a strategy to reduce life cycle GHG emission, microplastics and resource depletion." *Sustainability* 15, no. 15 (2023): 11529. https://doi.org/10.3390/su151511529

[4] Kabeyi, Moses Jeremiah Barasa, and Oludolapo Akanni Olanrewaju. "Review and Design Overview of Plastic Waste-to-Pyrolysis Oil Conversion with Implications on the Energy Transition." *Journal of Energy* 2023, no. 1 (2023): 1821129. https://doi.org/10.1155/2023/1821129

[5] Ibrahim, Idowu David, Yskandar Hamam, Emmanuel Rotimi Sadiku, Julius Musyoka Ndambuki, Williams Kehinde Kupolati, Tamba Jamiru, Azunna Agwo Eze, and Jacques Snyman. "Need for sustainable packaging: an overview." *Polymers* 14, no. 20 (2022): 4430. https://doi.org/10.3390/polym14204430

[6] Mansor, Wan Nurdiyana Wan, Nurul Ashraf Razali, Samsuri Abdullah, Mohammad Nor Khasbi Jarkoni, Anis Busrya Eddy Sharin, Nurul Huda Abd Kadir, Aima Ramli, How-Ran Chao, Sheng-Lun Lin, and Juliana Jalaludin. "A Review of Plastic-derived Diesel Fuel as a Renewable Fuel for Internal Combustion Engines: Applications, Challenges, and Global Potential." In *IOP Conference Series: Earth and Environmental Science*, vol. 1013, no. 1, p. 012014. IOP Publishing, 2022. https://doi.org/10.1088/1755-1315/1013/1/012014

[7] Ceviz, M. Akif, Bülent Çavuşoğlu, Ferhat Kaya, and İ. Volkan Öner. "Determination of cycle number for real in-cylinder pressure cycle analysis in internal combustion engines." *Energy* 36, no. 5 (2011): 2465-2472. https://doi.org/10.1016/j.energy.2011.01.038

[8] Paucar-Sánchez, Marco Favio, María Angeles Martín-Lara, Mónica Calero, Gabriel Blázquez, R. R. Solís, and Mario Jesús Muñoz-Batista. "Towards fuels production by a catalytic pyrolysis of a real mixture of post-consumer plastic waste." *Fuel* 352 (2023): 129145. https://doi.org/10.1016/j.fuel.2023.129145

[9] Jatadhara, Gollahalli Siddagangappa, Tumkur Krishnamurthy Chandrashekar, Nagaraj Ramalingayya Banapurmath, Nagesh Sampige Basavaraju, and Keerthi Kumar Nagaraja Setty. "Effect of Injection Timing in Direct Injection Diesel

Engine using Plastic Oil Diesel Blends with Biodiesel as an Additive." *Journal of Advanced Research in Fluid Mechanics and Thermal Sciences* 101, no. 2 (2023): 73-84. https://doi.org/10.37934/arfmts.101.2.7384

[10] Noor, Che Wan Mohd, Rizalman Mamat, Muhammad Yusri Ismail, Wan Nurdiyana, and Sheikh Alif. "Performance and Emission Control of Using Steam Injection on Medium Speed Marine Diesel Engine Running with Biodiesel Fuel." *Journal of Advanced Research in Fluid Mechanics and Thermal Sciences* 84, no. 2 (2021): 10-23.

[11] Chacón, Ana María Peco, Isaac Segovia Ramírez, and Fausto Pedro García Márquez. "K-nearest neighbour and K-fold cross-validation used in wind turbines for false alarm detection." *Sustainable Futures* 6 (2023): 100132. https://doi.org/10.1016/j.sftr.2023.100132

[12] Noor, Che Wan Mohd, Amirah Nur Fhatihah, Rizalman Mamat, Wan Mohd Norsani, Wan Nurdiyana, and Mohammad Nor Khasbi. "Properties study of B20 palm-methyl Ester biodiesel added with oxide nanoparticle towards green marine fuels." *Journal of Advanced Research in Applied Sciences and Engineering Technology* 29, no. 2 (2023): 212-222. https://doi.org/10.37934/araset.29.2.212222

[13] Rajendran, Silambarasan, and Pranesh Ganesan. "Experimental investigations of diesel engine emissions and combustion behaviour using addition of antioxidant additives to jamun biodiesel blend." *Fuel* 285 (2021): 119157. https://doi.org/10.1016/j.fuel.2020.119157

[14] Sunaryo, Sunaryo, Priyo Adi Sesotyo, Eqwar Saputra, and Agus Pulung Sasmito. "Performance and fuel consumption of diesel engine fueled by diesel fuel and waste plastic oil blends: An experimental investigation." *Automotive Experiences* 4, no. 1 (2021): 20-26. https://doi.org/10.31603/ae.3692

[15] Sekar, Manigandan, T. R. Praveenkumar, Veeman Dhinakaran, P. Gunasekar, and Arivalagan Pugazhendhi. "Combustion and emission characteristics of diesel engine fueled with nanocatalyst and pyrolysis oil produced from the solid plastic waste using screw reactor." *Journal of Cleaner Production* 318 (2021): 128551. https://doi.org/10.1016/j.jclepro.2021.128551

[16] Kaewbuddee, Chalita, Ekarong Sukjit, Jiraphon Srisertpol, Somkiat Maithomklang, Khatha Wathakit, Niti Klinkaew, Pansa Liplap, and Weerachai Arjharn. "Evaluation of waste plastic oil-biodiesel blends as alternative fuels for diesel engines." *Energies* 13, no. 11 (2020): 2823. https://doi.org/10.3390/en13112823

[17] Agu, Chinedu M., Kingsley A. Ani, Prince O. Abiazieije, Juliet A. Omeje, Jane C. Ekuma, Uchenna E. Umelo, Osondu H. Omukwu, Emeka D. Nwankwo, and Mmesoma P. Chinedu. "Biodiesel production from waste cat fish oil using heterogeneous catalyst from cat fish born: A viable waste management approach, and ANN modeling of biodiesel yield." *Waste Management Bulletin* 1, no. 4 (2024): 172-181. https://doi.org/10.1016/j.wmb.2023.11.002

[18] Bhatia, Shashi Kant, Ravi Kant Bhatia, Jong-Min Jeon, Arivalagan Pugazhendhi, Mukesh Kumar Awasthi, Dinesh Kumar, Gopalakrishnan Kumar, Jeong-Jun Yoon, and Yung-Hun Yang. "An overview on advancements in biobased transesterification methods for biodiesel production: Oil resources, extraction, biocatalysts, and process intensification technologies." *Fuel* 285 (2021): 119117. https://doi.org/10.1016/j.fuel.2020.119117

[19] Brzeziński, Mariusz, and Dariusz Pyza. "Carbon dioxide emission from diesel engine vehicles in intermodal transport." *Transport* 36, no. 3 (2021). https://doi.org/10.3846/transport.2021.15484

[20] Pilusa, Tsietsi Jefrey, Mansoor M. Mollagee, and Edison Muzenda. "Reduction of vehicle exhaust emissions from diesel engines using the whale concept filter." *Aerosol and Air Quality Research* 12, no. 5 (2012): 994-1006. https://doi.org/10.4209/aaqr.2012.04.0100

[21] Ağbulut, Ümit, Suat Sarıdemir, and Serdar Albayrak. "Experimental investigation of combustion, performance and emission characteristics of a diesel engine fuelled with diesel–biodiesel–alcohol blends." *Journal of the Brazilian Society of Mechanical Sciences and Engineering* 41, no. 9 (2019): 389. https://doi.org/10.1007/s40430-019-1891-8

[22] Nespeca, Maurilio Gustavo, Rafael Rodrigues Hatanaka, Danilo Luiz Flumignan, and José Eduardo de Oliveira. "Rapid and Simultaneous Prediction of Eight Diesel Quality Parameters through ATR-FTIR Analysis." *Journal of Analytical Methods in Chemistry* 2018, no. 1 (2018): 1795624. https://doi.org/10.1155/2018/1795624

[23] Kanchan, Sumit, Swastik Pradhan, Rajeev Kumar, Shubham Sharma, Omang Bhandari, Manisha Priyadarshini, Shashi Prakash Dwivedi *et al.,* "Developing a model for waste plastic biofuels in CRDi diesel engines using FTIR, GCMS, and WASPAS synchronisations for engine analysis." *Energy Exploration & Exploitation* 42, no. 2 (2024): 648-684. https://doi.org/10.1177/01445987231216762

[24] Sivashankar, M., G. Balaji, R. K. Barathraj, and V. Thanigaivelan. "Phenomena of brake specific fuel consumption and volumetric efficiency in CI engine by modified intake runner length." In *IOP Conference Series: Materials Science and Engineering*, vol. 402, p. 012086. IOP Publishing, 2018. https://doi.org/10.1088/1757-899X/402/1/012086

[25] Rajendran, Krishna Moorthy, Deepak Kumar, Bhawna Yadav Lamba, Praveen Kumar Ghodke, Amit Kumar Sharma, Leonidas Matsakas, and Alok Patel. "Effect of plasto-oil blended with diesel fuel on the performance and emission characteristics of partly premixed charge compression ignition engines with and without exhaust gas recirculation (EGR)." *Energies* 16, no. 9 (2023): 3750. https://doi.org/10.3390/en16093750

[26] Das, Subhadip, and Aniket Chowdhury. "An exploration of biodiesel for application in aviation and automobile sector." *Energy Nexus* 10 (2023): 100204. https://doi.org/10.1016/j.nexus.2023.100204

[27] Ali, Sheikh Alif, Anuar Abu Bakar, Chewanmn Wan, Khalid Samo Othman, Mohamad Nor Khasbi Jarkoni, Wan Nurdiyana Wan Mansor, and Md Redzuan Zoolfakar. "The NO_x Reduction Performances Of A Marine Diesel Engine Using Steam Induction Method For Blended Palm Oil Methyl Ester Fuel." *Journal of Engineering Science and Technology* 17, no. 4 (2022): 2904-2918.

[28] Mei, Hui, Lulu Wang, Menglei Wang, Rencheng Zhu, Yunjing Wang, Yi Li, Ruiqin Zhang, Bowen Wang, and Xiaofeng Bao. "Characterization of exhaust CO, HC and NOx emissions from light-duty vehicles under real driving conditions." *Atmosphere* 12, no. 9 (2021): 1125. https://doi.org/10.3390/atmos12091125